EARTH SURFACE PROCESSES AND LANDFORMS
Earth Surf. Process. Landforms **46**, 478–489 (2021)

Published online in Wiley Online Library
(wileyonlinelibrary.com) DOI: 10.1002/esp.5040

Robust methods for the decomposition and interpretation of compound dunes applied to a complex hydromorphological setting

Leon Scheiber,[1]* Oliver Lojek,[1] Axel Götschenberg,[2] Jan Visscher[1] and Torsten Schlurmann[1]
[1] Ludwig-Franzius-Institute for Hydraulic, Estuarine and Coastal Engineering, Leibniz University Hannover, Germany
[2] WSV – Federal Waterways and Shipping Administration, Wilhelmshaven, Germany

Received 17 February 2020; Revised 3 November 2020; Accepted 19 November 2020

*Correspondence to: Leon Scheiber, Ludwig-Franzius-Institute for Hydraulic, Estuarine and Coastal Engineering, Leibniz University, D-30167 Hannover, Germany.
E-mail: scheiber@lufi.uni-hannover.de

ESPL
Earth Surface Processes and Landforms

ABSTRACT: Underwater dunes are a morphological feature that are explored by marine scientists and coastal engineers alike. This study presents new methodologies in order to simplify bedform identification and morphodynamic analyses. Specifically, subaqueous compound dunes are decomposed with a simple yet extensive tracking algorithm, which relies on a repeated evaluation of unfiltered bed elevation profiles according to five predefined length classes. In a second step, morphological trends are assessed in the form of bed migration rates, bed slope asymmetries and net sediment changes, in which all parameters are referred to equidistant sections of the examined fairway stretch. This integrated approach not only avoids the challenges in weighting the varying size and abundance of dunes of different scales but also ensures comparability between dune-specific and areal parameters, which significantly improves the interpretation of the morphological setting as a whole. The developed methods are applied to the Outer Jade fairway, an anthropogenically influenced and regularly maintained waterway in the German Bight, and allow scrutiny of spatio-temporal trends in this region.

Based on a unique data set of 100 sequential high-quality echo-sounding surveys, various types of bedforms are identified, comprising large-scale primary as well as superimposing secondary dunes that are assumed to interfere with each other. Temporal trends show a long-term rise of the troughs of major bedforms and constant maximum crest elevations near the official maintenance depth, which matches the observed long-term aggradation of sediments. The spatial distribution of integrated morphodynamic parameters reflects a previously described zone of primary dune convergence and facilitates the precise localization of this geophysical singularity. The presented findings both confirm the robustness of the proposed methodologies and, in return, enhance the understanding of morphological processes in the Outer Jade. © 2020 The Authors. Earth Surface Processes and Landforms published by John Wiley & Sons Ltd.

KEYWORDS: bedform identification; German North Sea; Jade fairway; morphodynamics; subaqueous compound dunes

Introduction

Motivation

Subaqueous dunes are a remarkable morphological feature that can be found from the continental slopes (Reeder *et al.* 2011; Valentine *et al.*, 1984), over the bottom of tidal inlet channels (Ernstsen *et al.*, 2011; Zorndt *et al.*, 2011) to the beds of inland streams or rivers (Best, 2005; Parsons *et al.*, 2005). For more than a century, these bedforms have been the subject of scientific interest (Cornish, 1901) and were investigated by diverse working groups such as geologists, oceanographers and coastal engineers (Ashley *et al.*, 1990). By analogy with mutually interfering carrier and riding waves in transient sea states (Schlurmann, 2002), interaction of differing bedform types can be observed at so-called compound dunes consisting of large-scale primary and superimposing secondary dunes (Ashley *et al.*, 1990).

With regard to subaqueous dunes in estuarine settings, the motivation for bathymetric studies can originate from multiple objectives including the detection of unexploded ordnance devices, mapping of biota distributions or palaeohydraulic reconstructions, to name but a few. From an engineering perspective, understanding the prevailing morphological features and trends is also required to ensure the ease and safety of shipping in navigational channels. Accordingly, public authorities routinely monitor the bed level of tidal inlet channels and thus regularly observe sections that contain bedforms of all shapes and sizes that are possibly subjected to dredging activities in order to maintain fixed navigational depths. The corresponding echo-sounding data sets are readily available and can be a valuable basis for bedform-related studies as they comprise homogeneous and quality-controlled information about morphodynamic developments over a long period (e.g. Kubicki and Bartholomä, 2011; Zorndt *et al.*, 2011). Contrary to approaches that scrutinize predefined components of a filtered

bed profile (Aberle *et al.*, 2010; Frings and Kleinhans, 2008; Gehres *et al.*, 2013; Knaapen, 2005; van der Mark and Blom, 2007) or derive dune characteristics from spectral analyses (e.g. Cazenave *et al.*, 2013; Lefebvre *et al.*, 2011; Lisimenka and Kubicki, 2017; Winter and Ernstsen, 2007), the interest of local authorities is rather concentrated on absolute navigational depths and the physical properties of the sea floor. This comprises the existence of bedforms as well, since their growth and migration to shallower waters may cause major impediments to the ease and safety of shipping. It is therefore of importance to identify dune migration, its orientation and pathways, and other morphological trends to develop suitable sediment management strategies to sustain the waterway. The perspective of local shipping authorities towards subaqueous dunes, accordingly, can be summarized as a strictly phenomenological interest in a robust description of morphological features and trends, which is based on the raw sounding data of regularly conducted fairway surveys. The paper at hand presents and discusses results of such an engineering study that utilizes a recently investigated morphological setting, the Jade tidal inlet channel, to highlight the potential of two methodological suggestions: (1) a novel approach for the decomposition of compound dunes from unfiltered bed elevation profiles (BEPs) and (2) an assessment of morphological trends, which is decoupled from the dynamics of individual bedforms.

In particular, the newly developed dune identification algorithm returns a detailed description of prevailing dunes and their different heights and lengths, giving insight into the composition of compound dunes in the Jade tidal channel. The available data set also allows an analysis of both temporal and spatial trends regarding these dune dimensions and provides information for an attribution of the results. Furthermore, general morphodynamic trends can be addressed by an integrated assessment of predefined fairway sections. This approach not only avoids the challenges in weighting the different size and abundance of different bedforms but also ensures comparability between dune-specific (asymmetry/migration rate) and areal parameters (net sediment changes), which significantly improves the interpretation of the morphological setting as a whole. In doing so, the precise location of a postulated zone of dune convergence can be localized and long-term migration rates readily quantified.

Study area

The Jade is a tidally influenced embayment that cuts approximately 50 km into the marshland of Lower Saxony, a federal state in northern Germany. The water body is usually segmented into the Outer and the Inner Jade in the north as well as the Jade Bay in the south, where an eponymous river without notable freshwater discharge enters the tidal system (see Figure 1a,b). Destabilized by drainage and peat cutting, the Jade region was essentially formed during three consecutive extreme storm surges between 1509 and 1511 (Waldemar, 1979). With the Imperial Naval Port Act justifying the country's still biggest naval base in 1883, the Inner Jade was incrementally transformed into a transshipment complex hosting critical port infrastructure of national importance, creating the necessity for regular fairway maintenance (Akkermann *et al.*, 2015). The sedimentological inventory comprises medium and fine sands forming the navigational as well as other tidal channels and their respective sandbanks, while the intertidal flat areas contain silt (Valerius *et al.*, 2015). The morphological regime is governed by tides and waves as well as anthropogenic changes through construction and dredging activities. The semi-diurnal tides induce a tidal range between 2.8 m near Wangerooge at the northern end and 3.8 m at the narrow passage from the Inner Jade into the Jade Bay near Wilhelmshaven with current magnitudes exceeding 1.5 m s^{-1} (Grabemann *et al.*, 2004; Malcherek, 2010;

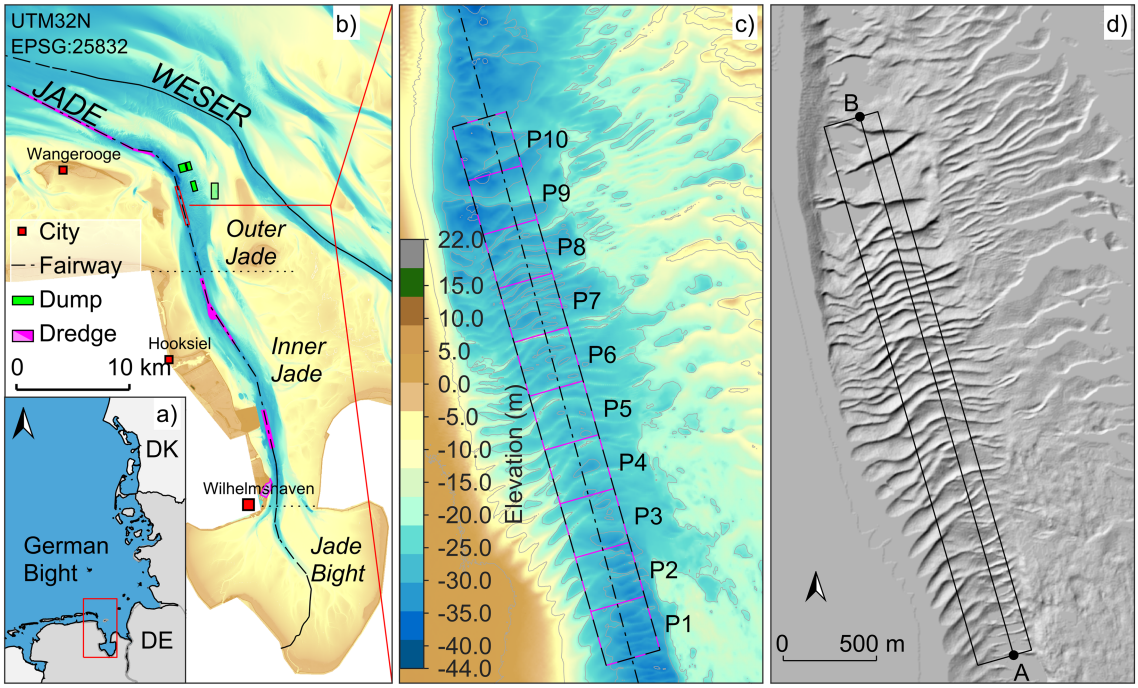

Figure 1. Study area: (a) German Bight and location of the Jade–Weser Estuary; (b) Jade–Weser Estuary bathymetry based on a composite from 2012 with indicated focus and adjacent maintenance areas; (c) dune field in the focus area with segmented investigation polygons; (d) hillshade representation of the dune field in part (c). [Colour figure can be viewed at wileyonlinelibrary.com]

Sündermann and Pohlmann, 2011). For the tidal channel, a net sediment import is reported, which stems from a seaward flood-dominated tidal asymmetry as well as from the negligible fresh water discharge and the geometry of the Jade Bay (Götschenberg and Kahlfeld, 2008; Lang, 2003). Owing to the importance of ensuring trustworthy conditions in the fairway channel, the existence of compound dunes is of particular interest, since dune crests oftentimes exceed the minimum water depth of -17.6 m chart datum (CD) and thus impede safe navigation towards the Jade Weser Port (JWP) and other supporting facilities. In cases where major dunes reach into the navigational channel and limit previously defined water depths, targeted water injection measures are conducted to effectively disperse their crest material into adjacent dune troughs. Far less often, trailing suction hopper dredgers are employed to thoroughly deepen sections of the fairway and deposit excess sediments at one of seven dump sites along the Jade.

In order to test the robustness of the proposed methodologies, the Jade presents a well-fitting test site given its long history of morphological studies (Reineck and Singh, 1967; Garrelts *et al.*, 1973; McLean, 1983; Ernstsen *et al.*, 2009; Svenson *et al.*, 2009). In particular, a dune field in the Outer Jade offers ample information about the existence of compound dunes that are known to contain bedforms of various sizes (Lefebvre *et al.*, 2011) and of a remarkable bathymetric feature, which is described as dune convergence (Kubicki and Bartholomä, 2011). Specifically, the combination of prevailing hydrodynamic conditions and the sedimentological inventory promote the formation of dunes that migrate on opposing trajectories and collide head-on at a particular location inside the navigational channel (Kubicki *et al.*, 2017). This unique setting is seen as a performance test for the aforementioned dune identification approach and integrated morphodynamic analyses. On the other hand, the introduced methodology enhances the understanding of morphological trends in this specific site.

Material and Methods

Data set

The dune convergence zone documented by Kubicki and Bartholomä (2011) is located in the northeastern German Bight between the opposing islands of Minsener Oog and Mellumplate comprising Jade fairway kilometres 29.0 and 32.0 (cf. Figure 1c). Monthly fairway soundings are available from the Waterways and Shipping Office (WSA) Wilhelmshaven with a regular resolution of 2 m × 2 m. Vessel-borne surveys are conducted with an *Atlas Fansweep 20-200* multi-beam echo-sounding (MBES) system that operates at a frequency of 200 kHz and achieves a vertical accuracy better than 0.05 m ± 0.2% of the water depth. Typical measurement duration for individual fairway sections spans 1–2 days and is tide independent. In total, 100 sequential surveys acquired between January 2010 and December 2018 were processed and analysed. The extent of the study site equals the intersection of all available surveys that cover the dune convergence zone. Along a fairway-parallel transect A–B (Figure 1d), BEPs with a discretization of 1.0 m were extracted from the survey data time series to further investigate dimensions and dynamics of prevailing bed features. The transect was chosen on the basis of statistic bedform occurrences, revealing the swath from 150 to 250 m (East–West) of the fairway to feature the highest number of bedforms.

Bedform identification

Prevailing bedforms were detected along the transects employing a simple and robust dune tracking approach, which was implemented in *MATLAB* (Versions: R2017a/R2019b, https://www.mathworks.com). Unlike other dune tracking tools (e.g. Gutierrez *et al.*, 2018; van der Mark and Blom, 2007), the algorithm employed in this study does not evaluate BEPs that are detrended or filtered in any way. In order to make allowance for the underlying, complex character of compound dunes in the focus area, it is instead based on an iterative identification of local extremes spaced in accordance with a widely accepted classification scheme proposed by (Ashley *et al.*, 1990). Depending on their length λ, bedforms can be categorized into ripples ($\lambda \leq 0.6$ m) as well as small ($0.6\,\text{m} < \lambda \leq 5\,\text{m}$), medium ($5\,\text{m} < \lambda \leq 10\,\text{m}$), large ($10\,\text{m} < \lambda \leq 100\,\text{m}$) and very large dunes ($100\,\text{m} < \lambda$). Respecting the available data resolution, the proposed algorithm performs the following three steps for each analysable length class: (1) find local extremes; (2) identify matching crest/trough pairs; (3) calculate dune dimensions:

1. The algorithm identifies local maxima along the bed elevation profile that have a prominence greater than a certain threshold value, while the identification of local minima is achieved analogously utilizing the inverted transect profile. To minimize subjectivity in the automated algorithm, the prominence threshold is defined as a fixed percentage of the theoretical mean dune height η at each class boundary derived from global regression results according to (Flemming, 1988).
2. In a second step, reasonable crest/trough pairs are assigned from the deduced catalogue of local extremes. For each tentatively tracked dune crest corresponding troughs are found at the closest adjacent minima. In accordance with thorough visual inspection, this methodology returns good results given the defined (class-specific) prominence thresholds. Critical exceptions to this approach occur wherever crest/trough pairs are incomplete, especially at the transect boundaries, which are therefore separated from the subsequent analysis.
3. Finally, dune dimensions are computed from the absolute position of crests and troughs for all echo-sounding surveys. Dune length, in this context, is taken as the absolute, i.e. in most cases not horizontal, distance between the two troughs that define a bedform. This procedure is necessary because no detrending of the BEPs is done beforehand and thus inclined bedforms are prevalent. Accordingly, dune heights have to be calculated from absolute distances as well, utilizing orthogonal trigonometric heights as proposed by (Wesseling and Wilbers, 2000) (cf. definitions in Figure 2b).

Although variation of the (one) calibration parameter results in partial changes regarding the total number of detected bedforms, especially at lower range values, sensitivity studies showed that spatial and statistical distributions remain qualitatively equal within the range of 5–25%. Higher values, in contrast, lead to an increasing neglect of small-scale bedforms and may cause obvious artefacts such as discontinuities in the resulting spectrum of bedform dimensions. For the present analysis, it was therefore decided to apply a universal height percentage of 15%, which represents a solid trade-off and ensures thorough dune detection. Moreover, small dunes and ripples were neglected within this study as a consequence of the limited horizontal resolution of the underlying data set (cf. Nyquist criterion) and the algorithm makes allowance for

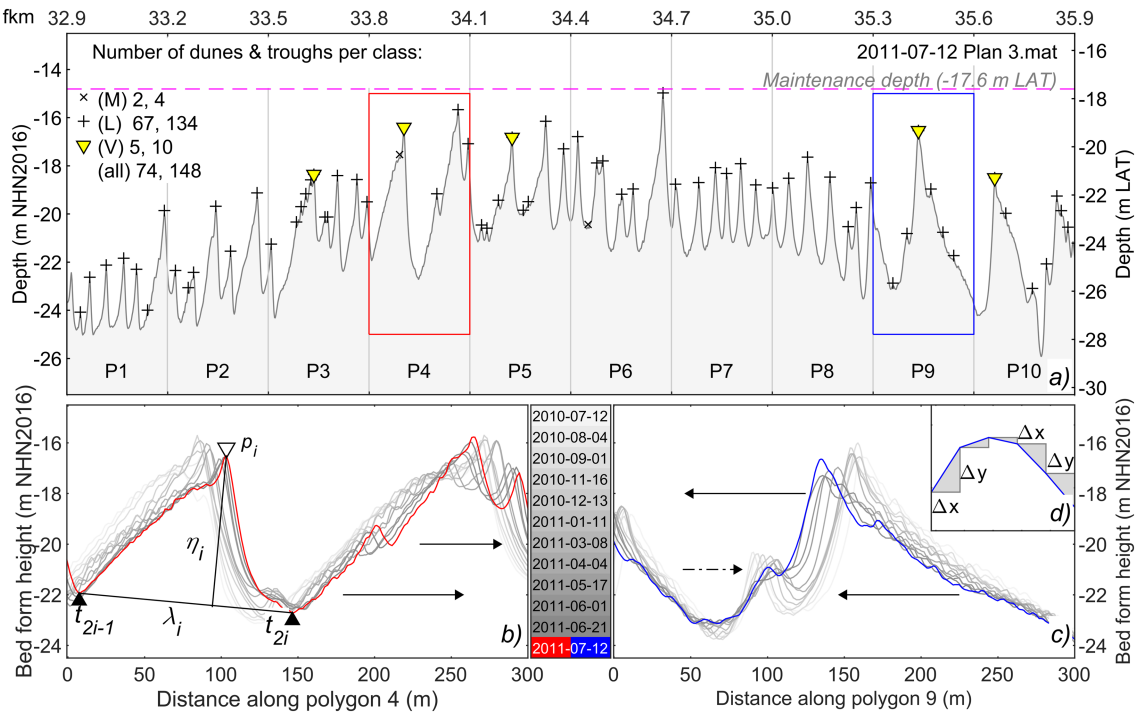

Figure 2. Applied methodology: (a) exemplary bed elevation profile along the transect A–B from July 2011 including number and position of identified bedform crests and troughs; (b) successive bed profiles within Polygon 4 and definition of dune dimension height and length; (c) migration of bed features in Polygon 9 as derived from maximum cross-correlations; (d) computation of bed asymmetries based on the ratio of positive and negative increment gradients. [Colour figure can be viewed at wileyonlinelibrary.com]

the limited vertical accuracy of the employed MBES device by omitting dunes with heights $\eta < 0.05$ m.

The general reliability of the outlined methodology was validated using a freely available MBES data set from Rio Paraná, Argentina, which was originally investigated by Parsons *et al.*, (2005). After detecting prevailing bedforms along a total of 150 longitudinal transects from a single (snapshot) bathymetry, dune dimensions and abundances were compared to results obtained from an analysis in accordance with the wavelet analysis tool developed by Gutierrez *et al.*, (2018) and those published in Cisneros *et al.*, (2020). Especially regarding the results of the former, the examination of this independent study area reveals good resemblance between the proposed and at least one established approach, except for the occurrence of outlying 'high small dunes' and 'low large or very large dunes', respectively, which are deemed critical by the authors. Although the juxtaposition of detection results allowed a first validation of the proposed methodology, it also raised questions regarding the comparability of available tools. A more detailed description of the validation scheme and its results is given as Supporting Information for this article.

Integrated morphodynamic parameters

Morphodynamics, on the other hand, were not computed for distinct bedforms but on the basis of fixed transect sections. This integrated methodology has several advantages over established methods when describing the general morphological setting of a study site, as the interpretation of dune-based parameters usually neglects the diverse size, abundance and dynamic behaviour of different bedform types. To make allowance for this problem, the Jade navigation channel offered a good opportunity to present an approach which is based on the independent morphodynamic parameters of bed asymmetry and bed migration rate.

For this purpose, the examined fairway segment was subdivided into equally spaced polygons of 300 m × 300 m each (cf. Figure 1c). The migration of bed features was then determined by cross-correlating the ten 300 m long profile sections of consecutive surveys (cf. Duffy and Hughes-Clarke, 2005). Figure 2b exemplifies the observed development of the fairway bed for Polygons 4 and 9 as grey shading. Bed migration rates u were derived from the relation between the average horizontal displacement (positive from South to North) and the time span elapsed between compared surveys.

Furthermore, bed asymmetries were analysed as a proxy for morphodynamic activity as commonly suggested for distinct dunes (e.g. Harris, 1991; Knaapen, 2005). The applied methodology is based on the following formula originally introduced by Zorndt *et al.*, (2011) for individual dunes:

$$A = \frac{N(\Delta y/\Delta x \leq 0) - N(\Delta y/\Delta x > 0)}{N(\Delta y/\Delta x)} \quad (1)$$

where x is the relative distance along the polygon, Δx is the inherent discretization length of 1 m, $\Delta y/\Delta x$ is the y-gradient at each discretization step and N is the number of steps greater/less than 0, respectively. The dimensionless bed asymmetry value A represents a dominance of positive bed inclinations (from South to North) if it ranges between −1 and 0, whereas negative inclinations are expressed in values $0 < A < 1$. A visualization of this approach is given in Figure 2c,d, where Polygon 9 exemplifies a bed section which is dominated by negative inclinations, i.e. relatively shorter southern slopes, and thus shows an asymmetry greater than 0. In this manner, polygon-specific migration rates and bed slope asymmetries were obtained for all surveys. Finally, morphodynamic changes were computed by means of a sediment volume balancing study for each polygon.

The obtained time series of class-related dune dimensions on the one hand and integrated bed dynamics on the other form the basis for a comprehensive analysis of the spatio-temporal

variation of bedforms in the Outer Jade navigation channel, as presented in the following.

Results

Dune characteristics

Examining all available BEPs resulted in an average number of about 92 detected bedforms along the 3000 m long fairway transect, ranging from medium to very large dunes. As can be seen from the logarithmic scatter plot in Figure 3, the corresponding dune dimensions reach values of up to 7.71 m in height and 260 m in length. The overall mean values amount to $\eta_{mean} = 1.58$ respectively. The distribution of these dune characteristics complies with maximum dimensions defined by a logarithmic function introduced by Flemming (1988). Comparing the average dune dimension ratio with these global values, the present study principally shows slightly higher dunes, which can be seen from a regression analysis depicted as a dash-dotted red line in Figure 3. The respective function for the Outer Jade reads as follows:

$$\eta_{mean} = 0.080 \cdot \lambda^{0.837} \quad (2)$$

Apart from the general over-representation of fully developed dunes, it is striking that dunes shorter than approximately 20 m do not reach their theoretical maximum heights. A second restriction of dune growth can be seen in the fact that very few bedforms exceed a height of 7.5 m notwithstanding their individual length. Moreover, sharp boundaries below 5.0 m length and 0.05 m height, respectively, reflect the constraints of data resolution, which preclude unambiguous identification of smaller bedforms.

An analysis of the long-term development of dune dimensions indicates that, throughout the analysed bedform classes, average heights were gradually shrinking over the 9-year survey period at annual rates of decrease of −0.95%, −0.35% and −3.1%, respectively (cf. trend lines in Figure 4a). Primary dune growth, suspected to cause the frequent shallowing of the Outer Jade fairway, could not be verified. Figure 4b contrasts the development of dune dimensions with an illustration of morphodynamic changes in the study area. The mean bed elevation of the examined fairway area covering 0.9 km^2 is characterized by fairly steady sediment accumulation especially after 2012; the comparison of mean bed levels before and after the survey period revealed an area-averaged aggradation of 0.955 mm^{-2}. In view of the described bedform developments, this finding suggests that sediment accumulation did not take place uniformly but was more intense near primary dune troughs, which resulted in a gradual levelling of the fairway bed profile, since crests exceeding the maintenance depth became subject to intervention. Figure 4b is complemented by bar plots representing annually dredged sediment volumes. Internal reports document that dredged mean volumes between 2013 and 2018 amounted to $6.3 \times 10^6 m^3$ for the comparably long fairway section fkm 36.0 to 39.0 captioned *Bypass of Minsener Oog* and $2.87 \times 10^6 m^3$ for fkm 18.0 to 24.0 (*Störtebecker Bank*), respectively. However, no dredging is reported for the documentation period regarding the fairway section examined within this study. Yellow bars, on the other hand, illustrate sediments that were disposed at one of the three nearest dump sites east of the focus area showing volumes up to 4.34×10^6 m^3 in the year 2016 (Federal Institute for Hydrology (BfG), 2020, Koblenz, Germany, in preparation). Overall, the fairway sections north and south of the examined dune field are continuously dredged, while dredged sediments, predominantly stemming from the Inner Jade, are dumped on spoil grounds east of the dune field (cf. Figure 1b). The cumulative dumping volume from these sites adds up to $15.54 \times 10^6 m^3$ for the years 2013 and 2018; the sediments accreting in the examined fairway section, in contrast, amount to approximately $0.84 \times 10^6 m^3$ during the same period equalling about 5%.

With respect to inherent statistical variations, Figure 5a gives an overview of the scatter of bedform heights within the applied dune classes. In this visualization, data on the *y*-axis is normalized using the individual mean heights η_{mean} as a reference for each of the four classes. Co-domains and 25th/75th percentiles are highlighted by light- and dark-blue shading in the background of each disintegrated dune class, respectively, and the underlying box plot is complemented by individual sample sizes. This methodology is repeated along the horizontal axis for each of the 10 sections of the transect, thus allowing insight into the spatial distribution of dune dimensions along the fairway. Figure 5b summarizes the average statistical variation within the three classes in equally normalized histograms. At first sight, this illustration suggests a relatively high probability

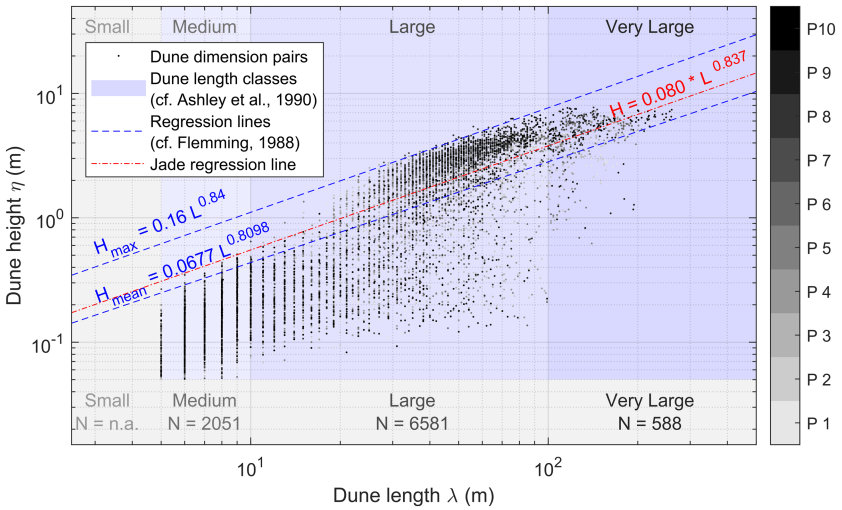

Figure 3. Dune dimensions: logarithmic scatter plot of dune dimension pairs identified by the dune tracking algorithm. The effective sampling sizes *N* comprise all bedforms of a specific dune class in accordance with the length scales introduced by Ashley *et al.* (1990). The dash-dotted regression line represents the mean height of dunes observed in the Outer Jade focus area, whereas the framing dashed lines are maximum and mean heights according to global reference data reported by (Flemming, 1988). [Colour figure can be viewed at wileyonlinelibrary.com]

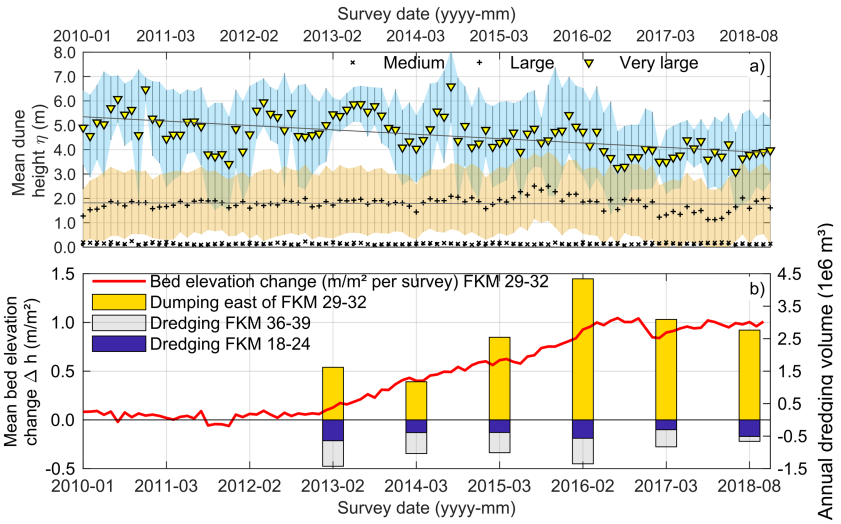

Figure 4. Temporal trends: (a) evolution of mean dune heights, related to the four dune length classes, over the assessed period between January 2010 and December 2018 and complemented by colour-shaded standard deviations; (b) long-term mean bed elevation changes for the complete focus area and annual dredging volumes for the adjacent fairway stretches. [Colour figure can be viewed at wileyonlinelibrary.com]

of occurrence for large dunes. However, this effect is related to the definition of this intermediate class rather than to the relative frequency of lengths, since corresponding class boundaries relate to $-0.816 \cdot \sigma$ and $+1.816 \cdot \sigma$ deviations from the overall mean dune length, respectively. This peculiarity has some further implications on the statistics of dune dimensions: whereas very large dunes can be seen as almost normally distributed, large dunes in the Outer Jade show a bimodal distribution. This observation becomes clearer in view of the previous Figure 3. With respect to heights, the majority of large dunes in this case can be assigned to one of two groups, namely either fully developed (long) dunes, which appear to be normally distributed as well, or shorter dunes, which are not fully developed. These latter dunes mostly show heights below 0.5 m, hence densely occupying the four smallest frequency bins. The interjacent height range between 0.8 and 1.8 m, in contrast, is sparsely represented. The remaining class of medium dunes is again normally distributed, which is due to the exclusive occurrence of not fully developed dunes, although the distribution exposes a certain skewness as a result of the predefined minimum height boundary. Among the analysed bedform classes, large dunes show the broadest range of corresponding heights, with several extremes reaching almost fourfold the reference value η_{mean}. The highlighted percentiles are mainly bound to the boundaries of ±50% of each specific height.

Also in consideration of the spatial variation of bedform heights, it should be distinguished between large and very large dunes on the one hand and medium dunes on the other. The distributions of the two former types suggest a segmentation of the fairway into a southern and a northern half, which is reflected in the ranking of median dune heights: apparently the highest large and very large dunes can be found in the seaward direction. Given the relatively sheltered location of the southern polygons behind the island of Minsener Oog,

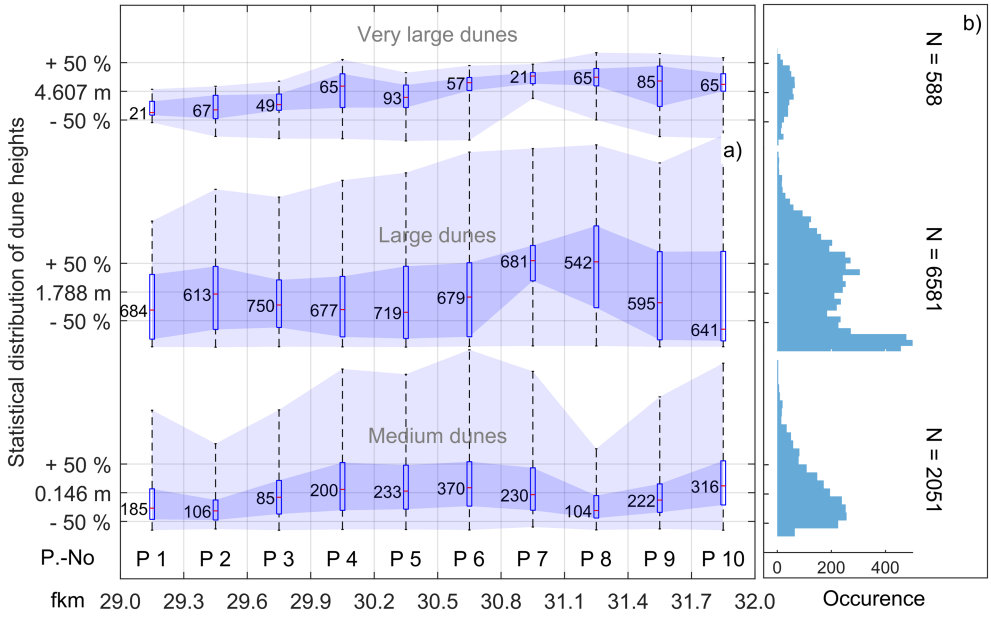

Figure 5. Spatial trends: distribution of bedform heights according to the length classification proposed by Ashley *et al.* (1990): (a) normalized height variation within length classes versus spatial distribution along the fairway transect; (b) normalized histograms of dune heights within the four classes. [Colour figure can be viewed at wileyonlinelibrary.com]

this observation indicates the existence of two unequal hydrodynamic regimes. Medium dunes, in contrast, show a different trend: these bedforms show both highest median values and maximum abundance in the central third of the transect, which suggests an increasingly complex character of compound dunes in this area.

Morphodynamic developments

The Hovmöller diagram in Figure 6 illustrates the bed elevations along the fairway transect in a greyscale map. A graphical composition of consecutive surveys along the *y*-axis allows deeper insights into the development of these elevation profiles in space and time. Apart from the faintly observable influence of five major campaigns of fairway maintenance, highlighted as dash-dotted lines in Figure 6, the general morphodynamic trends of this fairway transect become evident when focusing on the lightest grey contours, which can be interpreted as primary dune crests. In detail, Polygons 1–6 are characterized by up to five large to very large dunes. The inclination of these and smaller, interjacent bedforms demonstrates the northward migration of this part of the channel bed. In contrast, the northernmost sections of the transect, i.e. Polygons 8–10, comprise between two and four primary dunes with reverse inclinations and thus evidently migrate southward. The only part of the examined fairway without clearly inclined crest levels appears in Polygon 7, where almost no migration can be observed throughout the complete time span of data acquisition. These findings suggest that prevailing bed features between fkm 29.0 and 32.0 migrate head-on and that the region of dune convergence can be detected close to the survey polygon 7.

Further support for this observation was derived from cross-correlations and an examination of bed asymmetries. Figure 7 depicts the spatial distribution of these two polygon-specific parameters along the fairway. Specifically, overall mean values are represented by solid lines, whereas dotted annual means indicate the corresponding temporal range of values. For the analysed period, mean migration rates vary between $4.6\,\mathrm{cm\,d^{-1}}$ in Polygon 1 and $-3.5\,\mathrm{cm\,d^{-1}}$ in Polygon 10, where positive signs epitomize northward and negative signs southward migration, respectively. The corresponding annual means show extreme values of $9.4\,\mathrm{cm\,d^{-1}}$ and $-6.7\,\mathrm{cm\,d^{-1}}$, respectively. An average bandwidth of $\pm 3.1\,\mathrm{cm\,d^{-1}}$ implies rather little variation between the individual years. In general, the mean migration rates are steadily decreasing from South to North with a zero-crossing at Polygon 7. South of this change in direction, migration rates average out at +3.65 cm $\mathrm{d^{-1}}$ ($\hat{=}13.3\,\mathrm{m\,yr^{-1}}$), north of the zero-crossing at $-1.93\,\mathrm{cm\,d^{-1}}$ ($\hat{=}\ -\ 7.1\,\mathrm{m\,yr^{-1}}$). As with the spatial distribution of dune characteristics before, the fact that migration rates crucially differ between southern and northern polygons, yielding a ratio of nearly 1:−2, indicates the existence of residual currents opposing with equal magnitudes. This finding corroborates the present understanding of a singular hydrodynamic setting causing head-on dune collision in the Outer Jade.

With regard to bed slope asymmetries, annual and overall means show an analogous trend with the difference of the inverse definition of this parameter. The extremes of annual mean bed asymmetries are found in Polygon 2 ($A = -0.33$) and Polygon 9 ($A = +0.31$), respectively. Overall mean values vary between −0.24 (Polygon 4) and +0.14 (Polygon 9); the average bandwidth amounts to ±0.11. Except for the two boundary polygons, the overall mean asymmetries show steadily increasing values from South to North.

In conclusion, both graphs profoundly underscore the observations from Figure 6 and show mostly positive inclinations, i.e. presumably northward orientation, for the fairway reach between fkm 29.0 and 30.8. The northern part of the study area (fkm 31.1 and 32.0), in contrast, is characterized by dominating negative inclinations. Both parameters change their orientation in Polygon 7, which can be linked to the indicated zone of dune convergence. This area, therefore, can be traced to the fairway section between fkm 30.8 and 31.1. With respect to local morphodynamics, this is also the region where net sediment transport rates were minimal or even negative for the investigated survey period.

A temporal analysis of migration rates and bed asymmetries does not exhibit any significant long-term trends. However, it became apparent that major shifts in magnitude and even direction of both parameters coincided with the cyclone season. Examples of such changes were observed in the aftermath of recent European windstorms, such as 'Xaver' in December 2013 or the storm cluster 'Elon & Felix' in January 2015, but not further scrutinized within this paper.

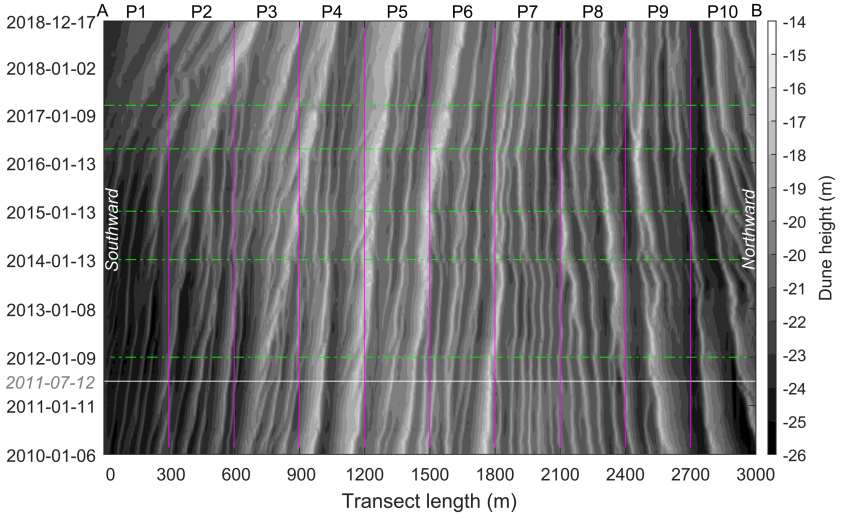

Figure 6. Hovmöller diagram: visualization of bed dynamics along the detrended fairway transect A–B between January 2010 and December 2018 in a Hovmöller diagram. Note the white profile from July 2011, which was introduced in Figure 2 before, as well as suspected occasions of water injection measures highlighted by dash-dotted green lines. [Colour figure can be viewed at wileyonlinelibrary.com]

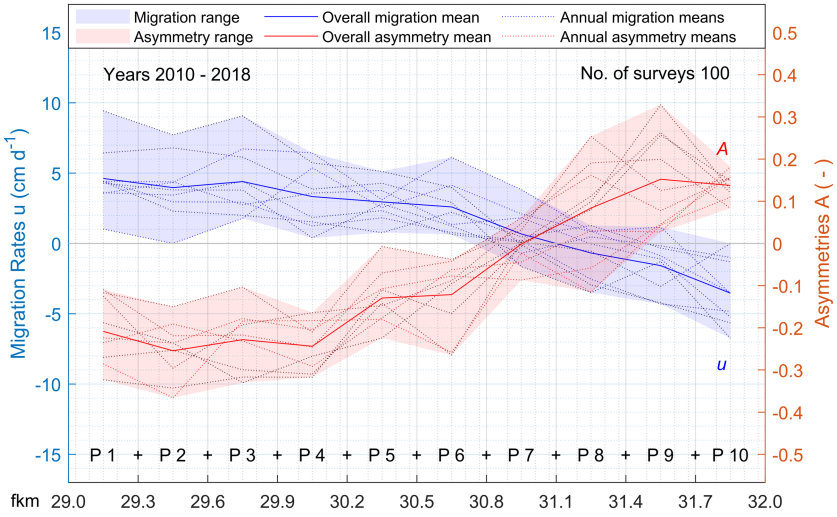

Figure 7. Migration convergence: spatial distribution of the morphodynamic parameters, bed migration rates and bed slope asymmetries. Solid lines represent the overall mean values inside the 10 transect sections, whereas dotted lines and patches indicate the temporal variation between individual years. [Colour figure can be viewed at wileyonlinelibrary.com]

Discussion

Recent studies have indicated a unique hydrodynamic setting causing a head-on convergence of large-scale bedforms (Kubicki and Bartholomä, 2011; Kubicki *et al.*, 2017). This as well as a general public interest in enhancing the current sediment management strategy presented an opportunity to apply new methodologies for both the decomposition and comprehensive evaluation of compound dunes and an assessment of general morphodynamic trends along a fairway-parallel transect.

Compound dunes in the Outer Jade

The iterative application of the newly developed algorithm facilitated the identification of a broad and dense spectrum of dune dimension tupels that are generally in line with global mean data collected by Flemming (1988). The presented double-logarithmic plot (Figure 3) also suggests that dunes in the tidally influenced waters do not exceed a maximum *relative* height of about 7.5 m. Referring this length-independent value to the local water depths that range from −25 m to −20 m height/depth ratios yield 1:0.3–0.375, which matches a standard value of $\eta < h/3$ reported by Zanke (2013) (for a compilation of historical ratios see also Zanke, 1982). It is therefore concluded that the growth of very large dunes is limited by the local water depth. However, this finding does not preclude the artificial reduction of *absolute* dune heights in the context of water injection measures, which could also be observed especially in the central, shallower parts of the focus area.

In addition, the conducted analyses suggest that dunes in the Outer Jade can be subdivided into two different types, namely fully developed (mainly $\lambda > 20$ m) and not fully developed ($\lambda < 20$ m) ones. Closer inspection of the evaluated BEPs confirms that the latter are in general independent bedforms and equivalent to those instantly perceivable by eye (cf. Figure 2a). On the other hand, shorter dunes are typically superimposed on the slopes of these primary dunes and thus notably inclined by analogy with the behaviour of carrier and riding waves (Schlurmann, 2002). These geometric scales are generally in line with compound dunes investigated in other estuarine settings (Dalrymple *et al.*, 1978; Villard and Kostaschuk, 1998). The suppressed development of secondary dunes, derived from a kink in the distribution of dune dimension ratios in Figure 3, is assumed to be a consequence of the hydrodynamic boundary conditions affecting these superimposing bedforms. Apart from their inclined alignment, this fact might be connected to shadowing or wake effects behind larger primary dunes. What is more, this type of bedform contains relatively small sediment volumes and thus is more subjected to the impact of the tidal currents (that reverse twice per day) than primary dunes, which was described for secondary dune heights in the Inner Jade (Ernstsen *et al.*, 2009) or dune asymmetries in comparable tidal environments (Winter *et al.*, 2008) before. Secondary dune heights, accordingly, seem to persist in a quasi-steady state here, which is characterized by semi-diurnal fluctuations. Results obtained for these dune classes are consequently highly dependent on the precise tidal phase during which the bathymetric data were obtained. Unfortunately, no such information is available for the presented data set and therefore no well-founded interpretation can be given regarding the short-term reworking or hysteresis of these dunes at the moment. Constraints also apply for spatial scales, so that secondary dune dimensions currently convey a mainly qualitative character. Nevertheless, the methodology is generally applicable to all dune classes from smallest-scale ripples to very large dunes provided that bathymetric data are available at a sufficient temporal and spatial resolution.

The two described dune types can also be retraced statistically within the three analysed length classes, in which the class of large dunes is particularly noteworthy, since it contains both types of dune as a kind of mode mixing effect. This results in a bimodal height frequency distribution, which is perceptible in other data sets as well but not interpreted as such (e.g. Lisimenka and Kubicki, 2019; Van der Mark *et al.*, 2007). From the present analysis it is concluded that large dunes in the Outer Jade are either large-scale primary dunes or superimposing and relatively shorter secondary dunes riding on the carrying, i.e. primary dunes. The bimodal probability density, hence, is attributed to the prevailing hydrodynamic conditions on the one hand and the choice of classification intervals on the other.

Although recent investigations suggest that sediment from adjacent dump sites is continuously transported into the Outer Jade fairway (Scheiber *et al.*, 2019), linear regressions for the temporal development of dune dimensions analytically attest to the long-term reduction of mean dimensions for most dune classes. This outcome has to be seen against the background of recurring anthropogenic interference in this area. Local authorities regularly disperse dune crests through water injection measures transferring bed material into the dune troughs and thus artificially reducing the relative height of bedforms. This effect could be observed in surface plots (3D) and transects

(2D) from successive soundings on several occasions (e.g. Figure 6). In the long run, this practice results in an overall aggradation and consequently in a reduction of the mean water depth (until capital dredging activities become inevitable). Current practices, therefore, are considered suitable on a medium-term timescale, as they ensure safe navigational conditions, but not sustainable in the long run.

Considering the spatial distribution of primary dune heights along the transect, the fairway can be divided into two parts, namely a southern part, where mostly moderate dune dimensions prevail, and a morphologically more active northern part with increased dune dimensions adjoining the open sea. Complemented by results stemming from a sediment volume balancing study, this finding corroborates the idea of two independent and opposing residual currents in these areas, which provoke a zone of dune convergence as presented by Kubicki *et al.*, (2017). Additionally, height distributions and probabilities for medium dunes indicate an increasing complexity of compound dunes in the central part of the transect with its centre in Polygon 7. This observation supports the idea of an area, which is characterized by the convergence of compound dunes.

Local morphodynamic trends

The broached assumption was further substantiated by an analysis of morphodynamic parameters using a Hovmöller diagram to facilitate an initial evaluation of the complex spatio-temporal development of bed features along the transect. The diametrical inclination of major crests and troughs, herein, strikingly reflects the suggested head-on migration converging between fkm 30.8 and 31.1. This trend is even more pronounced for the spatial distribution of morphodynamic parameters, which both show a zero crossing in this area. Interestingly, this is the very part of the fairway where net transport volumes were minimal or even negative during the sample period. Considering previously published results of a simulation of residual current patterns, this observation holds true given that the head-on migration of bed features is driven by two independent currents until the transported bed material is redirected by a cross-fairway flow component, namely the superposition of two counter-rotating net current vortices (Kubicki *et al.*, 2017).

Bedform identification

The presented study develops and utilizes a novel bedform tracking algorithm that allows the decomposition of subaqueous compound dunes and thus a comprehensive analysis of their interfering components. Depending on the available data resolution, identified bedforms can range from small-scale ripples to very large dunes of several hundreds of metres in length. Unlike other dune tracking approaches, the applied methodology relies on an iterative evaluation of unfiltered BEPs according to the established length classification proposed by Ashley *et al.*, (1990). The approach was applied for the following three reasons: it is simple, unbiased and exhaustive.

The showcased algorithm successfully detected primary and secondary bedforms along the Outer Jade fairway notwithstanding their stacked alignment and the rather complex hydro- and morphodynamic setting. Reducing the methodological steps and resorting to basic *MATLAB* functions ensures that the algorithm is easy to replicate and, what is more, employed straightforwardly. The obtained locations and dimensions of prevailing bedforms subsequently allow further analyses in any systematic research study. As a consequence of the oftentimes complex character of subaqueous dunes, many other bedform identification routines demand certain assumptions and require mathematical predefinitions, as to which range of wavelengths is of interest. Once collected BEPs are then detrended by the use of either moving average (van der Mark and Blom, 2007) or bandpass filters (Gutierrez *et al.*, 2018) in order to isolate the signal component of interest, while altering the original profile through the application of (subjective) filter criteria. Even if the definition of a focus wavelength is carefully chosen, this procedure necessarily entails an underestimation of identified bedform heights, since absolute profile amplitudes are systematically reduced. In this regard, the validation for bedforms at the Paraná river showed that, although statistical parameters like median and mean dune lengths corresponded for the proposed and existing tracking algorithms, the respective dune heights were reduced by up to 50% (see Supporting Information for more details). This becomes problematic, wherever the exact height of compound dunes is more important than their (theoretically inherent) components, for example when monitoring the morphodynamic developments along a fairway. For this reason, it was key to develop an algorithm that processes unfiltered BEPs and avoids any user-induced bias, which was realized in the form of a repeated search for local extremes. The choice of a reasonable focus wavelength was standardized by the global definition of five established dune classes and the same number of evaluation runs for each bed elevation profile. In this manner the entirety of comprised bedforms can be identified even in the case of compound dunes and without modifications, i.e. detrending or filtering, to the original elevation profile. This is worth noting, as many other approaches are not exhaustive, or at least it is unclear under what circumstances these algorithms obtain a complete spectrum of included bedforms without redundant identification of dunes. The validation scheme also brought to light the existence of certain artefacts, especially near the co-domain boundaries, as a by-product of some alternative methodologies, whereas others showed questionable discontinuities. It should be noted, though, that both external algorithms employed for the comparison are currently still under development. Given the multitude and diversity of existing dune tracking routines, it will be an essential objective for future studies to systematically investigate the assets and drawbacks of all available approaches.

One potential shortcoming of the presented approach can be seen in the mode mixing effects observed for the class of large dunes. This length category represents a disproportionate percentage of the overall spectrum, which, for the Outer Jade data set, results in a bimodal frequency distribution that combines (physically different) primary and secondary dunes. Future investigations should re-evaluate this point considering a subdivision of this length class or investigating ways to determine the natural (site-specific) boundary length between the two dune types beforehand; the presented methodology provides a good starting point for such objectives. Alternatively, it may be expedient to formulate an independent set of bandpass limits originating from the data set instinctively following the methods known as ensemble empirical mode decomposition (EEMD) (Dätig and Schlurmann, 2004; Huang *et al.*, 1998; Wu and Huang, 2009). Further limitations arise from the decision to focus on a single longitudinal section out of a three-dimensional bathymetry: apart from the challenging definition of this representative transect, all cross-fairway components are necessarily neglected by this approach. Although homogeneous alignment of dune crests and mostly linear migration allows this simplification in the Outer Jade (as it is also applicable in many other areas), a refinement towards an autonomous determination of an interrogation line, which is based on the statistical orientation of crests, would crucially

enhance the objectivity of the described algorithm; this feature could also be used to allow for curved bathymetries. The reliance on a proprietary *MATLAB* function for the computation of local extreme values may be seen as a third shortcoming, since it limits the domain of potential users and may obscure full understanding of the underlying workflow. Nevertheless, this cross-reference makes the described methodology comparable and much easier to replicate, and this limitation is therefore accepted as a compromise until a more objective but still simple approach is found.

In conclusion, systematically assessing BEPs with respect to the suggested bedform length classes yields reasonable results and allows a decomposition and comprehensive analysis of compound dunes while keeping the unbiased MBES signal. Although still subject to certain shortcomings, the introduced methodology is expedient and ensures easy application and replication.

Integrated morphodynamic analyses

After successfully describing the prevailing dunes along the transect, morphodynamic trends were scrutinized by assessing slope asymmetries and migration rates. Although typically referring to individual bedforms, both parameters were replaced by generalized values describing 10 equidistant sections of the fairway. The length of these sections was chosen in excess of the maximum dune dimensions and in view of the surveyed channel width. The resulting square polygons also facilitate a comparison between volumetric sediment changes on the one hand and section-specific parameters on the other, which can be seen as representative given the mostly cross-fairway alignment of bed features.

Classical, dune-specific migration rates are computed from the displacement of critical points of a bedform that is observed at two different time steps; this can be accomplished by calculating the displacement of peaks and troughs (Knaapen *et al.*, 2005) or cross-correlating the complete signal (Duffy and Hughes-Clarke, 2005). This procedure fails wherever a correct attribution of corresponding dunes is not possible, i.e. with calving and merging dunes or at the profile boundaries. Moreover, an automation of this approach becomes critical if migration between consecutive surveys exceeds the length of examined bedforms (e.g. Masselink *et al.*, 2009). In the present case, where survey intervals can exceed 1 month and deformation of dunes is ubiquitous, these flaws were avoided by conducting cross-correlations for each of the fixed polygons and thereby decoupling migration trends from distinct dunes. Although precise information about individual bedforms is neglected by this approach, it still resembles a focus on large-scale primary dunes as presented in other studies (e.g. Bartholdy *et al.*, 2002; Kubicki *et al.*, 2017), albeit without the described attribution problems. In fact, the proposed polygon or binning approach even supports the understanding of the examined dune field as a whole and therefore qualifies for all study sites, at which general migration pathways are under consideration.

Replacing readily available dune asymmetries by bed slope related values along the fairway sections shares several of the aforementioned advantages/disadvantages, for instance, when it comes to the weighting of dune-specific features. Small and large dunes naturally show very different dynamics as a consequence of their abundance, size and alignment (Ernstsen *et al.*, 2009). For the present data set, the volatility of small-scale dunes causes significant attenuation of the general morphodynamic trends, raising the question of which dune classes reflect the overall setting best. The use of bed slope asymmetries is employed to allow for this problem in an objective way and, eventually, also ensures that migration, sediment transport and bed inclination are comparable. The approach can therefore be seen as a useful component of the suggested analysis of general morphodynamic trends, as required for the localization of dune convergence in the Outer Jade and other locations, even if dune-specific information is neglected.

Finally, it is again noted that strategic fairway maintenance in regard to navigational depths or sediment balances does not necessarily rely on the dynamics of individual bedforms, especially if they are part of a larger and complex system governed by multiple stressors and anthropogenic influence, but on the correct interpretation of trends. Morphodynamical developments, however, can also go beyond mere sediment accumulation or erosion, and to this effect the introduced parameters allow valuable insights into general migration rates and trajectories. Even if specific limitations may preclude their application in more fundamental studies, several engineering objectives seem virtually predestined for the presented methodology.

Conclusion

Subaqueous compound dunes are a remarkable bathymetric feature that can be of importance to diverse research topics as well as for engineering practice, such as the operation and maintenance of public waterways. Based on a case in the German North Sea, the paper at hand presents new methodologies to interpret this phenomenon in a simple yet extensive way. Specifically, a newly developed algorithm is showcased that ensures a robust decomposition of compound dunes comprised in an unfiltered bed elevation profile. The methodology was validated beforehand by comparison with established dune tracking approaches utilizing parallel transects of a single (snapshot) bathymetry from Rio Paraná, Argentina. Secondly, an approach is introduced that allows a generalized evaluation of morphodynamic developments such as migration rates and pathways inside the complex field of dunes.

The study site is located between fkm 29.0 and 32.0 of the Outer Jade navigation channel, where previous surveys suggested a zone of head-on dune migration. A unique echo-sounding data set from 100 successive navigational safety surveys conducted between January 2010 and December 2018 allowed a comprehensive analysis into the morphodynamic processes in this area. Bed elevation profiles derived from a 3000 m long transect along the available fairway section were used to test the iterative application of the novel dune tracking approach, which is based on a widely accepted categorization of bedform lengths. A dense and continuous spectrum of dune dimension tupels and their strong resemblance to global results from the literature corroborates the robustness of the applied methodology. On average, the semi-automated algorithm identified some 92 medium to very large dunes per survey along the fairway transect. The respective dune dimensions range from minimum values near the constraints of accuracy and resolution to maximum lengths of 260 m and maximum heights of 7.71 m, respectively, in which numerous very large dunes appear to be height restricted by the available water depth. Moreover, class-related mean dimensions show decreasing trends over the assessed period at constant absolute crest levels but rising troughs. This is explained by regular water injection measures applied to excess dune crests resulting in a constant levelling of the fairway bed and long-term aggradation. Accordingly, the fairway bed inside the study area is characterized by extensive sediment accumulation amounting to +0.955 $m\,m^{-2}$ over 9 years. Moreover, a previously discussed zone of dune convergence is reflected in the spatial distribution of dune

dimensions. This trend is even more pronounced with regard to the morphodynamic characteristics of bed migration and bed slope asymmetries, as both parameters show a change of direction between fkm 30.8 and 31.1. The average celerity of opposing bed features was computed as $+13.3\,\mathrm{m\,yr^{-1}}$ from South to North and $-7.1\,\mathrm{m\,yr^{-1}}$ in the opposite direction. In this way, the discussed zone of dune convergence could be verified and precisely located within this study.

In conclusion, it was possible to confirm the robustness of both the iterative application of a length class-related dune tracking approach and the analysis of integrated morphodynamic parameters on the basis of transect sections by applying them to a dune field under complex hydromorphological conditions and reproducing previous findings. What is more, the introduced methodologies even enhanced the understanding of morphodynamic processes in the focus area and qualify for future employment, especially in the field of applied coastal research.

Acknowledgements—The authors wish to thank the WSA Wilhelmshaven for providing the echo-sounding data sets forming the foundation for this study. Furthermore, the authors are grateful for the collaboration and support from the BAW on early-stage developments of the methods presented here.

Conflicts of Interest

The authors declare that they do not have any conflicts of interest.

Acronyms

BAW	Federal Waterways Engineering and Research Institute
BEPs	bed elevation profiles
BfG	Federal Institute for Hydrology
CD	chart datum
DTMs	digital terrain models
EEMD	Ensemble Empirical Mode Decomposition
fkm	fairway kilometre
JWP	Jade Weser Port
MBES	multi-beam echo-sounding
WSA	Waterways and Shipping Office
WSV	Waterways and Shipping Administration

Symbols

λ	bedform length (m)
η	bedform height (m)
p_n	bedform peak (–)
t_n	bedform trough (–)
Δx	horizontal distance increment (m)
Δy	vertical distance increment (m)
A	bed slope asymmetry (–)
u	bed migration rate ($\mathrm{cm\,d^{-1}}$)

Data Availability Statement

The MBES data sets of the Outer Jade used and analysed during the current study are available from the WSA Wilhelmshaven on reasonable request. Bathymetric data of the Rio Paraná, which were used for a validation of the introduced dune tracking approach, is provided as an exemplary file of the *Bedforms Analysis Toolkit for Multiscale Modeling* (BedformsATM) developed by (Gutierrez *et al.*, 2018). Complementary bedform results for this region were carefully extracted from a database hosted by the University of Illinois at Urbana–Champaign (Cisneros, 2020). Exemplary code for the presented dune tracking approach is available from the corresponding author on request.

References

Aberle J, Nikora V, Henning M, Ettmer B, Hentschel B. 2010. Statistical characterization of bed roughness due to bed forms: a field study in the Elbe river at Aken, Germany. *Water Resources Research* **46**(3): W03521. https://doi.org/10.1029/2008WR007406

Akkermann R, Brunken H, Michaelsen W, Moritz V, von Essen L-M. 2015. *Die Jade: Flusslandschaft am Jadebusen: landes- und naturkundliche Beiträge zu einem Fluss zwischen Moor, Marsch und Meer*. Isensee: Oldenburg.

Ashley G, Boothroyd JC, Bridge JS, Clifton HE, Dalrymple R, Elliott T, Flemming B, Harms JC, Harris P, Hunter RE, Kreisa RD, Lancaster N, Middleton GV, Paola C, Rubin DM, Smith JD, Southard JB, Terwindt JHI, Twitchell DC. 1990. Classification of large-scale subaqueous bedforms: a new look at an old problem. *Journal of Sedimentary Petrology* **60**: 160–172.

Bartholdy J, Bartholomä A, Flemming BW. 2002. Grain-size control of large compound flow-transverse bedforms in a tidal inlet of the Danish Wadden Sea. *Marine Geology* **188**(3–4): 391–413.

Best J. 2005. The fluid dynamics of river dunes: a review and some future research directions. *Journal of Geophysical Research: Earth Surface* **110**(F4): F04S02.

Cazenave P, Dix J, Lambkin D, McNeill L. 2013. A method for semi-automated objective quantification of linear bedforms from multi-scale digital elevation models. *Earth Surface Processes and Landforms* **38**: 221–236. https://doi.org/10.1002/esp.3269

Cisneros J. 2020. Data for: Dunes in the world's big rivers are characterised by low-angle leeside slopes and a complex shape. https://doi.org/10.13012/B2IDB-7525764_V2

Cisneros J, Best J, Van Dijk T, de Almeida RP, Amsler M, Boldt J, Freitas B, Galeazzi C, Huizinga R, Ianniruberto M, Ma H, Nittrouer JA, Oberg K, Orfeo O, Parsons D, Szupiany R, Wang P, Zhang Y. 2020. Dunes in the world's big rivers are characterized by low-angle leeside slopes and a complex shape. *Nature Geoscience* **13**(2): 156–162.

Cornish V. 1901. On sand-waves in tidal currents. *The Geographical Journal* **18**(2): 170–200.

Dalrymple RW, Knight RJ, Lambiase JJ. 1978. Bedforms and their hydraulic stability relationships in a tidal environment, Bay of Fundy, Canada. *Nature* **275**(5676): 100–104.

Dätig M, Schlurmann T. 2004. Performance and limitations of the Hilbert–Huang transformation (HHT) with an application to irregular water waves. *Ocean Engineering* **31**(14–15): 1783–1834.

Duffy GP, Hughes-Clarke JE. 2005. Application of spatial cross correlation to detection of migration of submarine sand dunes. *Journal of Geophysical Research: Earth Surface* **110**: F04S12. https://doi.org/10.1029/2004JF000192

Ernstsen VB, Winter C, Becker M, Bartholdy J. 2009. Tide-controlled variations of primary and secondary bedform height: Innenjade tidal channel (Jade Bay, German Bight). In *6th IAHR Symposium on River, Coastal and Estuarine Morphodynamics: RCEM*; 779–786.

Ernstsen VB, Lefebvre A, Bartholdy J, Bartholomä A, Winter C. 2011. Spatiotemporal height variations of large-scale bedforms in the Grådyb tidal inlet channel (Denmark): a case study on coastal system impact. *Journal of Coastal Research*: 746–750.

Federal Institute for Hydrology (BfG). (2020) Unterbringung von Baggergut aus der Unterhaltungsbaggerung auf die Unterbringungsstellen in der Jade - Untersuchung nach GÜBAK. Internal report commissioned by the Waterways and Shipping Office Weser-Jade-Nordsee. Koblenz, BfG-2019.

Flemming BW. 1988. Zur Klassifikation subaquatischer, strömungstransversaler Transportkörper. *Bochumer geologische und geotechnische Arbeiten* **29**: 93–97.

Frings R, Kleinhans M. 2008. Complex variations in sediment transport at three large river bifurcations during discharge waves in the river Rhine. *Sedimentology* **55**: 1145–1171. https://doi.org/10.1111/j.1365-3091.2007.00940.x

Garrelts E, Harten H, Hovers G, Lucht F, Oebius H, Ohlmeyer F, Rohde H, Sindern J, Vollmers H-J, Wigand V. 1973. *Die Ausbauten der Mündungsstrecken der deutschen Tideströme und deren Einfluß auf die Sandbewegung*, 23. Internationaler Schifffahrtskongreß. Deutsche Beiträge: Ottawa. July 1973.

Gehres N, Qrefa-Sander M, Entelmann I, Winterscheid A. 2013. *Dynamics of sub-aquatic bed form structures in the Tidal Elbe, Northern Germany*, Vol. **1242**. EGU General Assembly 2013: Vienna, Austria. 7–12 April 2013.

Götschenberg A, Kahlfeld A. 2008. *The Jade*. Boyens: Heide, Holstein. Die Küste 74; 263–274.

Grabemann H-J, Grabemann I, Eppel DP. 2004. Climate change and hydrodynamic impact in the Jade–Weser area: a case study. *Coastline Reports* **1**: 83–91.

Gutierrez RR, Mallma JA, Núñez-González F, Link O, Abad JD. 2018. Bedforms-ATM, an open source software to analyze the scale-based hierarchies and dimensionality of natural bed forms. *SoftwareX* **7**: 184–189.

Harris PT. 1991. Reversal of subtidal dune asymmetries caused by seasonally reversing wind-driven currents in Torres Strait, Northeastern Australia. *Continental Shelf Research* **11**(7): 655–662. https://doi.org/10.1016/0278-4343(91)90018-2

Huang NE, Shen Z, Long SR, Wu MC, Shih HH, Zheng Q, Yen N-C, Tung CC, LiuProc HH. 1998. The empirical mode decomposition and the Hilbert spectrum for nonlinear and non-stationary time series analysis. *Proceedings of the Royal Society of London, Series A* **454**: 903–995.

Knaapen MAF. 2005. Sandwave migration predictor based on shape information. *Journal of Geophysical Research: Earth Surface* **110** (F4): F04S11. https://doi.org/10.1029/2004JF000195

Knaapen MAF, van Bergen Henegouw CN, Hu YY. 2005. Quantifying bedform migration using multi-beam sonar. *Geo-marine Letters* **25** (5): 306–314.

Kubicki A, Bartholomä A. 2011. Sediment dynamics in the Jade tidal channel prior to port construction, Southeastern North Sea. *Journal of Coastal Research*: 771–775.

Kubicki A, Kösters F, Bartholomä A. 2017. Dune convergence/divergence controlled by residual current vortices in the Jade tidal channel, South-Eastern North Sea. *Geo-Marine Letters* **37**(1): 47–58. https://doi.org/10.1007/s00367-016-0470-6

Lang G. 2003. Ein Beitrag zur Tidedynamik der Innenjade und des Jadebusens. *Mitteilungsblatt der Bundesanstalt für Wasserbau* **86**: 33–42.

Lefebvre A, Ernstsen V, Winter C. 2011. Bedform characterization through 2D spectral analysis. *Journal of Coastal Research*: 781–785.

Lisimenka A, Kubicki A. 2017. Estimation of dimensions and orientation of multiple riverine dune generations using spectral moments. *Geo-Marine Letters* **37**(1): 59–74.

Lisimenka A, Kubicki A. 2019. Bedload transport in the Vistula River mouth derived from dune migration rates, Southern Baltic Sea. *Oceanologia* **61**(3): 384–394.

Malcherek A. 2010. *Gezeiten und Wellen*. Vieweg+Teubner: Wiesbaden. https://doi.org/10.1007/978-3-8348-9764-0

Masselink G, Cointre L, Williams J, Gehrels R, Blake W. 2009. Tide-driven dune migration and sediment transport on an intertidal shoal in a shallow estuary in Devon, UK. *Marine Geology* **262**(1–4): 82–95. https://doi.org/10.1016/j.margeo.2009.03.009

McLean SR. 1983. Turbulence and sediment transport measurements in a North Sea tidal inlet (the Jade). In *North Sea Dynamics*, Sündermann J (ed), Springer: Berlin; 436–452.

Parsons DR, Best JL, Orfeo O, Hardy RJ, Kostaschuk R, Lane SN. 2005. Morphology and flow fields of three-dimensional dunes, Rio Paraná, Argentina: results from simultaneous multibeam echo sounding and acoustic Doppler current profiling. *Journal of Geophysical Research: Earth Surface* **110**(F4).

Reeder DB, Ma BB, Yang YJ. 2011. Very large subaqueous sand dunes on the upper continental slope in the South China Sea generated by episodic, shoaling deep-water internal solitary waves. *Marine Geology* **279**(1–4): 12–18.

Reineck HE, Singh IB. 1967. Primary sedimentary structures in the recent sediments of the Jade, North Sea. *Marine Geology* **5**(3): 227–235.

Scheiber L, Lojek O, Visscher J, Melling G. 2019. Potential drivers for primary dune growth in the Outer Jade. In *Proceedings of the International Conference on Marine and RiverDune Dynamics 2019*, Lefebvre A, Garlan T, Winter C (eds). MARUM – Center for Marine Environmental Sciences, University Bremen and SHOM: Bremen, Germany; 207–211.

Schlurmann T. 2002. Spectral analysis of nonlinear water waves based on the Hilbert–Huang transformation. *Journal of Offshore Mechanics and Arctic Engineering* **124**(1): 22–27. https://doi.org/10.1115/1.1423911

Sündermann J, Pohlmann T. 2011. A brief analysis of North Sea physics. *Oceanologia* **53**(3): 663–689. https://doi.org/10.5697/oc.53-3.663

Svenson C, Ernstsen VB, Winter C, Bartholomä A, Hebbeln D. 2009. Tide-driven sediment variations on a large compound dune in the Jade tidal inlet channel, southeastern North Sea. *Journal of Coastal Research* **1**: 361–365.

Valentine PC, Cooper RA, Uzmann JR. 1984. Submarine sand dunes and sedimentary environments in Oceanographer Canyon. *Journal of Sedimentary Research* **54**(3): 704–715.

Valerius J, Kösters F, Zeiler M. 2015. Erfassung von Sandverteilungsmustern zur großräumigen Analyse der Sedimentdynamik auf dem Schelf der Deutschen Bucht: AufMod. *Die Küste* **83**: 39–63.

van der Mark CF, Blom A. 2007. A new and widely applicable bedform tracking tool. Civil Engineering and Management Research Reports 2007R-003/WEM-002; No. 1568-4652). Enschede: Water Engineering & Management (WEM).

Van der Mark CF, Blom A, Hulscher SJMH. 2007. Variability in bedform characteristics using flume and river data. In *River, Coastal and Estuarine Morphodynamics: RCEM 2007*, Dohmen-Janssen CM, Hulscher SJMH (eds), Taylor & Francis: Leiden; 923–930.

Villard P, Kostaschuk R. 1998. The relation between shear velocity and suspended sediment concentration over dunes: Fraser Estuary, Canada. *Marine Geology* **148**(1–2): 71–81.

Waldemar R. 1979. *Küstenentwicklung und Deichbau während des Mittelalters zwischen Maade, Jade und Jadebusen*, Sonderdruck. Ostfriesische Landschaft: Aurich, Germany.

Wesseling C, Wilbers AWE. 2000. Manual DT2D version 2.3: Software for dune-tracking in two dimensions.

Winter C, Ernstsen VB. 2007. Spectral analysis of compound dunes. In *River, Coastal and Estuarine Morphodynamics: RCEM 2007*, Dohmen-Janssen CM, Hulscher SJMH (eds), Taylor & Francis: Leiden; 907–911.

Winter C, Vittori G, Ernstsen VB, Bartholdy J. 2008. On the superimposition of bedforms in a tidal channel. *Marine and River Dune Dynamics*: 337–344.

Wu Z, Huang NE. 2009. Ensemble empirical mode decomposition: a noise-assisted data analysis method. *Advances in adaptive data analysis* **1**(01): 1–41.

Zanke U. 1982. *Grundlagen der Sedimentbewegung*. Springer: Berlin. https://doi.org/10.1007/978-3-642-68660-3

Zanke UC. 2013. *Hydromechanik der Gerinne und Küstengewässer: Für Bauingenieure, Umwelt- und Geowissenschaftler*. Springer: Berlin.

Zorndt AC, Wurpts A, Schlurmann T. 2011. The influence of hydrodynamic boundary conditions on characteristics, migration, and associated sand transport of sand dunes in a tidal environment. *Ocean Dynamics* **61**(10): 1629–1644.

